

Article

The Role of Physical Parameterizations on the Numerical Weather Prediction: Impact of Different Cumulus Schemes on Weather Forecasting on Complex Orographic Areas

Giuseppe Castorina ^{1,2}, Maria Teresa Caccamo ^{1,2}, Franco Colombo ^{2,3} and Salvatore Magazù ^{1,2,*}

¹ Department of Mathematical and Informatics Sciences, Physical Sciences and Earth Sciences (MIFT), University of Messina, Viale F. Stagno D'Alcontres 31, 98166 Messina, Italy; gcastorina@unime.it (G.C.); mariateresa.caccamo@unime.it (M.T.C.)

² CISFA—Interuniversity Consortium of Applied Physical Sciences, 98123 Messina, Italy; franco.colombo@aeronautica.difesa.it

³ Italian Air Force Meteorological Service—Comando Aeroporto, 95030 Sigonella, Italy

* Correspondence: smagazu@unime.it

Abstract: Numerical weather predictions (NWP) play a fundamental role in air quality management. The transport and deposition of all the pollutants (natural and/or anthropogenic) present in the atmosphere are strongly influenced by meteorological conditions such as, for example, precipitation and winds. Furthermore, the presence of particulate matter in the atmosphere favors the physical processes of nucleation of the hydrometeors, thus increasing the risk of even extreme weather events. In this framework of reference, the present work aimed to improve the quality of weather forecasts related to extreme events through the optimization of the weather research and forecasting (WRF) model. For this purpose, the simulation results obtained using the WRF model, where physical parametrizations of the cumulus scheme can be optimized, are reported. As a case study, we considered the extreme meteorological event recorded on 25 November 2016, which affected the whole territory of Sicily and, in particular, the area of Sciacca (Agrigento). In order, to evaluate the performance of the proposed approach, we compared the WRF model outputs with data obtained by a network of radar and weather stations. The comparison was performed through statistical methods on the basis of a “contingency table”, which allowed for ascertaining the best suited physical parametrizations able to reproduce this event.

Keywords: WRF model; air quality; extreme weather conditions; physical parametrizations; convective phenomena; contingency table



Citation: Castorina, G.; Caccamo, M.T.; Colombo, F.; Magazù, S. The Role of Physical Parameterizations on the Numerical Weather Prediction: Impact of Different Cumulus Schemes on Weather Forecasting on Complex Orographic Areas. *Atmosphere* **2021**, *12*, 616. <https://doi.org/10.3390/atmos12050616>

Academic Editors: Yun Zhu, Jim Kelly, Jun Zhao, Jia Xing and Yuqiang Zhang

Received: 7 April 2021

Accepted: 6 May 2021

Published: 11 May 2021

Publisher's Note: MDPI stays neutral with regard to jurisdictional claims in published maps and institutional affiliations.



Copyright: © 2021 by the authors. Licensee MDPI, Basel, Switzerland. This article is an open access article distributed under the terms and conditions of the Creative Commons Attribution (CC BY) license (<https://creativecommons.org/licenses/by/4.0/>).

1. Introduction

The optimization of meteorological models is very important in the prediction of the genesis of extreme weather events. In the limited area models (LAM) and particularly in the weather research and forecasting (WRF) model, the physical parameterization of convective phenomena plays a fundamental role in a good simulation of the dynamics of the atmosphere. The physical processes associated with the condensation of water vapor are essentially non-linear, and therefore their overall effect can directly influence large-scale circulation.

In this framework, the Sicilian territory is characterized by extreme weather events that frequently cause flash floods [1]. During these episodes, the precipitations occurring in few hours often exceed the rain accumulations that normally occur in several months.

These extreme precipitations are usually connected with intense and quasi-stationary mesoscale convective phenomena that insist on the same area for several hours. However, they occur at a local scale (microscale) and hence a fruitful approach requires a deep convection parameterization. Their intensity is often determined by local factors such as

the presence of orographic reliefs close to the coastline. The upward movement of the air on the windward side of a mountain range (known as the Stau effect) facilitates the formation of clouds and rain. Adiabatic expansions and compressions are well-known examples of thermodynamic processes and have recently been investigated also through the R uchardt experiment [2] and the frequency analysis procedure [3].

Sicily, due to its geographical position and its complex orographic morphology, is often interested in extreme weather events. Being at the center of the Mediterranean Sea, Sicily is in the transition zone between the arid and dry climate of North Africa and the more temperate and moist climate of central Europe, and hence it is often affected by those phenomena that are triggered by the interactions between processes typical of middle latitudes and tropics [4–6]. In the early autumn months, the seas surrounding Sicily are normally affected by Mediterranean cyclones [7,8] that originate from the contrast between air masses with very different temperatures and moisture [9], which interact with the high-temperature marine water (sea surface temperature, SST). These conditions can cause extreme weather events characterized by sudden and heavy rainfalls and dangerous flash floods. In the summertime, between May and September, the thermo-convective thunderstorm affects the inland areas of Sicily, where temperature can reach very high values [10,11].

One of the most important challenges of meteorological modeling is to develop models that can predict with high rates of success, both the time and the place where a convective cell start to develop as well as their evolution in time and space [12,13].

In recent years, several advances have been made on this purpose, and the limited area models, nowadays used in the major computing centers, are often able to provide an answer with adequate accuracy [14,15].

The weather research forecast (WRF) model is a numerical weather prediction system designed for research needs and operational forecasting of weather phenomena.

This model is the result of a collaborative effort between the National Center for Atmospheric Research (NCAR), the National Centers for Environmental Prediction (NCEP), and the Earth System Research Laboratory (ESRL) of the National Oceanic and Atmospheric Administration (NOAA). The WRF is designed both for scientific purposes (for example for the numerical simulations of the atmospheric dynamics) and for applicative purposes, such as numerical weather predictions.

Furthermore, it is possible to implement the model through the optimization of an integrated system based on the WRF model coupled with the chemistry module (WRF–Chem). It consists of a type of “online” model as it allows for the emission, transport, dispersion, transformation, and sedimentation of all anthropogenic and natural pollutants [16,17]. In the latter case, for example, it is possible to consider both physical processes and chemical transformations of aerosol particles released during volcanic eruptions. Indeed, it is worth noting that, although weather conditions are the main factor that determines the air quality, they depend on the direct and indirect effects that chemical compounds have on solar radiation and cloud microphysics [18].

The results of these simulations were obtained using the weather research and forecasting (WRF) model, version 3.7.1. [19], specifically optimized for Sicily, which is a territory with a complex orography [20–22].

For the sake of the improvement of the model performance, some progress has been made in the understanding of the mechanisms governing the formation and the localization of convective systems capable of producing large quantities of precipitation [23,24].

In particular, the physical parameterizations concerning the convective phenomena have been improved [25]. The parameterization of convective phenomena plays a fundamental role in a good simulation of the dynamics of the atmosphere. The physical processes associated with the condensation of water vapor are essentially non-linear, and therefore their overall effect can directly affect large-scale circulation. [26,27].

In this framework, the study has been addressed to seek the best model configurations capable of giving the best weather forecasting [28].

The case study treated in the work concerns the extreme meteorological event that took place on 25 November 2016, which has interested the entire territory of Sicily (see Figure 1), in particular the area of Sciacca (Agrigento). In this event, the observed precipitation was purely convective, and therefore it is advisable to compare the numerical forecasts as the convective schemes vary. To evaluate the performance of the model simulations, we performed statistical analyses using the pluviometric data provided for by the model and the daily precipitation observed by 13 weather stations provided by the network of the Regional Department of Civil Protection (DRPC) of Sicily.

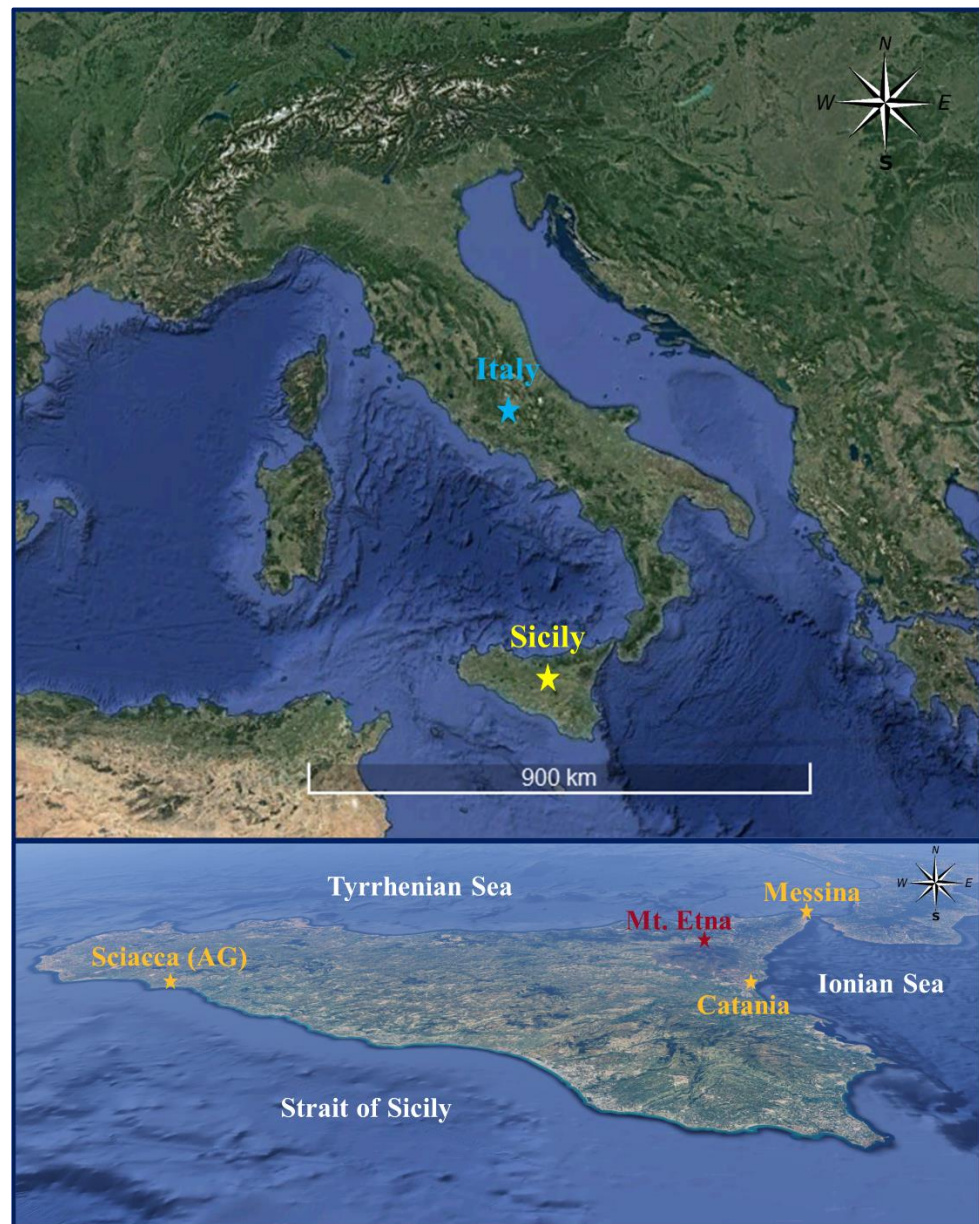


Figure 1. Top panel: map showing the location of Sicily in Europe. Bottom panel: Detail of Sicily showing the geographical position of the cities of Messina, Catania, and Sciacca; the seas; and Mount Etna.

2. Description of the Case Study

2.1. Synoptic Analysis

November 2016 was characterized by a long and prolonged phase of bad weather that affected the whole of Sicily. Due to its intensity, the event that occurred on the 25th of November was one of the most significant, causing spread floods both on the southern

coast and on the Ionian coast between the towns of Catania and Messina. Large-scale vertical movements were favored by the presence of a 500 hPa vortex located above Spain (see Figure 2).

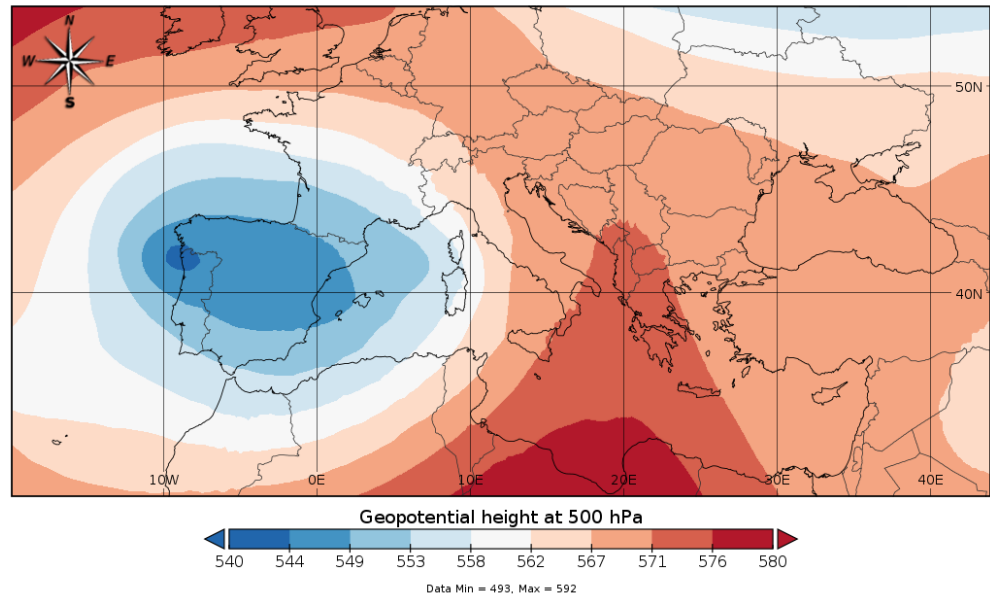


Figure 2. Geopotential at 500 hPa. The synoptic analysis shows a depression vortex located on the Iberian Peninsula.

This baric configuration attracted intense flows of southern currents towards Sicily. These southern flows carried large quantities of moisture released by the Libyan Sea, which have been interested in high surface temperatures (close to 20 °C, see Figure 3). However, on the west of Sicily, the air flows were oriented from the western quadrants, and the post-frontal air masses were colder. Therefore, there were simultaneously the presence of three components able to generate the initial development of a convective system: the presence of a high level of moisture in the lower atmosphere; the sea surface temperature still relatively high, capable of providing latent heat during condensation processes; and, finally, instability of the troposphere [29,30].

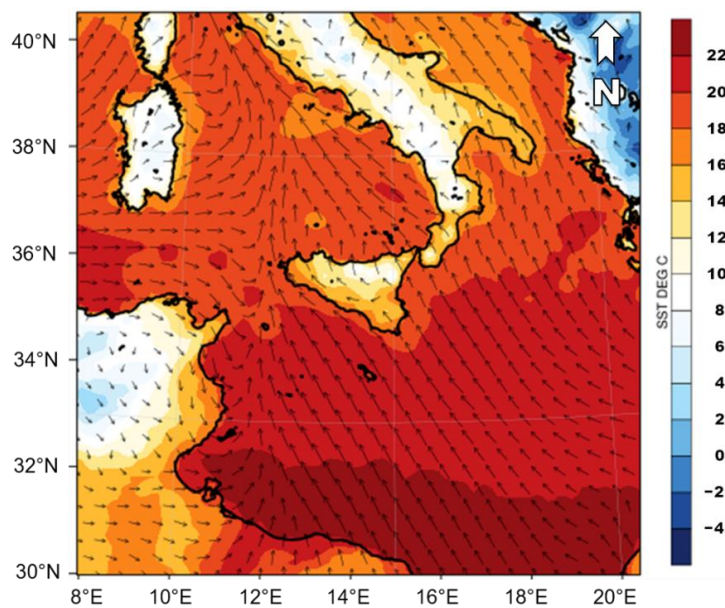


Figure 3. Analysis of SST and surface wind currents. The figure shows the high temperatures of the sea surface that favors the increase of the moisture of the air masses that fly over them.

In the hours immediately following 00:00, the first cold air impulses reached the western coasts of Sicily, initially causing thunderstorms to spread in the Trapani area. The frontal lifting operated by the arrival of the cold air mass found an environment already favorable to the trigger of a strong convective storm. The storm line gave rise to a huge V-shaped storm that developed just to the north of the island of Pantelleria, affecting all of the western parts of Sicily with intense rainfall, particularly the southern coast between the towns of Ribera and Sciacca (see Figure 4).

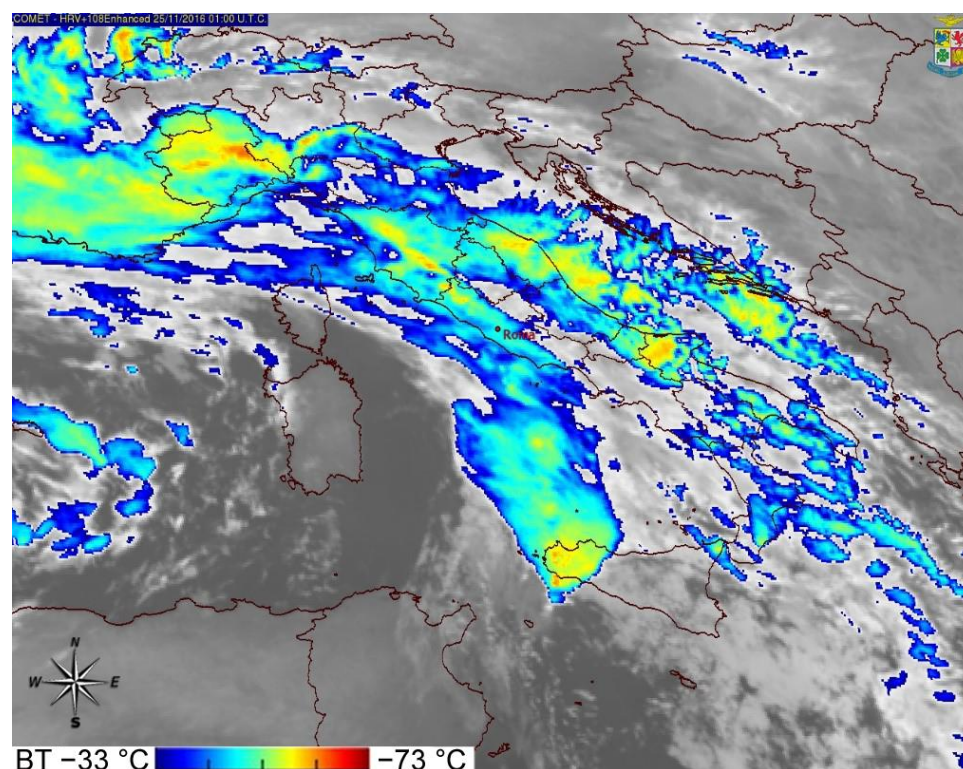


Figure 4. MSG enhanced nephoanalysis of 25.11.2016 at 01:00 UTC.

These so-called V-shaped thunderstorms were mesoscale storm systems with the characteristic of producing intense precipitations in the southern portion of the V point where super cellular elements could be active [31,32]. About 200 mm of rainfall was recorded by the weather station of Bivona between 05:30 and 11:00 UTC, with maxima values of 51.4 mm in 30 min. The weather station of Giuliana, a few kilometers west of Bivona, recorded 163.2 mm. In the same hours, severe precipitations affected also the eastern coast, producing a flood in the town of Giardini Naxos.

2.2. WRF Model

The numerical simulation of this case study was carried out using the weather research and forecasting (WRF) model. The advanced research WRF (ARW) modeling system was adopted. Figure 5 shows the numerical domain adopted in the present work. Figure 6 shows the orography of the domain under examination. The horizontal space of the grid was 5 km in both directions with 65 vertical levels up to 50 hPa. The initial and boundary conditions were acquired by the global model global forecast system (GFS) at 0.25 degrees with a time interval resolution of 1 h processed starting from the 00Z run relative to 24 November 2016. The real-time global sea surface temperature analysis (RTG-SST) with a resolution of 0.083 degrees was used. For long-wave and short-wave radiations, the rapid radiative transfer model for GCM (RRTMG) scheme was used. In addition, the above models were also used the schemes of Mellor–Yamada–Janjic for the boundary layer and the Noah land surface model. The microphysical scheme utilized was the Thompson, a well-known double-moment scheme widely tested especially for high-resolution simulations.

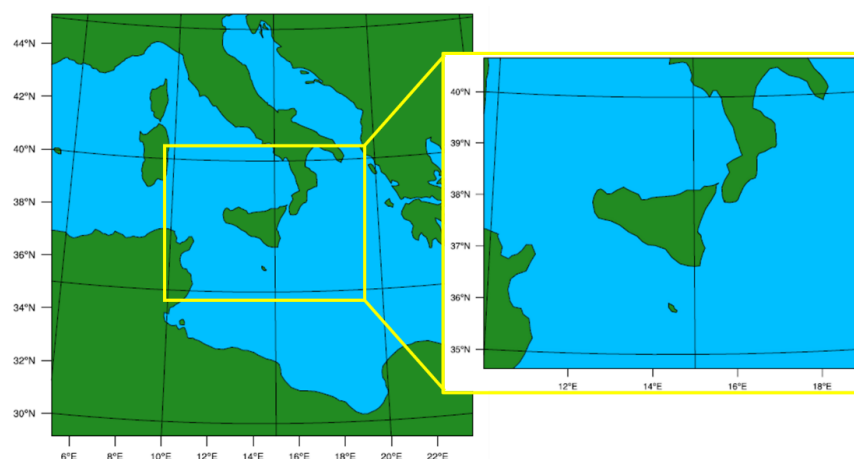


Figure 5. Map of the spatial domain used by the WRF model. The domain is centered in Sicily. The model is configured with a horizontal grid spacing of 5 km and a time interval resolution of 1 h.

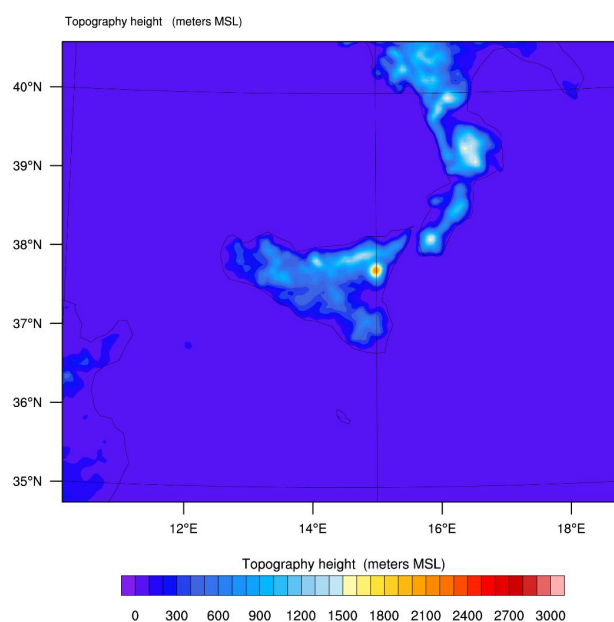


Figure 6. Topographical height (expressed in meters above sea level) of the domain under examination.

3. Results and Discussion

The study carried out in this work concerns the evaluation of the performance of the WRF model when different cumulus parameterizations are applied [33]. In particular, the forecasts of the spatial distribution of rain during the extreme event were compared. The parameterizations compared are the follows: CU0 represents the explicit convection; CU1 is the Kain–Fritsch scheme [34,35], which is a deep and shallow convection sub-grid scheme, using a mass flux approach with downdrafts and convective available potential energy (CAPE) removal time scale; CU2 is the Betts–Miller–Janjic scheme and it is an operational Eta scheme [36,37] and a column moist adjustment scheme relaxing towards a well-mixed profile; CU3 is the Grell–Devenyi (GD) scheme, an ensemble scheme involving a multi-closure, multi-parameter, ensemble method with typically 144 sub-grid members; CU5 is the Grell 3D scheme, which is an improved version of the GD scheme that may also be used on high resolution (in addition to coarser resolutions) if subsidence spreading (option `cugd_avedx`) is turned on [38]; CU6 is the Tiedtke scheme, which is a mass-flux type scheme with CAPE removal time scale, shallow component, and momentum transport; finally, CU14 is the new simplified Arakawa–Schubert scheme [39], a new mass-flux scheme with deep and shallow components and momentum transport.

Figure 7 shows the total rainfall accumulations (accumulate + convective) obtained from the WRF model simulations when the physical parameterizations of the convective schemes vary (Figure 7a–g). The results obtained were compared with the map of data observed by the network of meteorological stations by the Regional Department of Civil Protection (DRPC) of Sicily (Figure 7h).

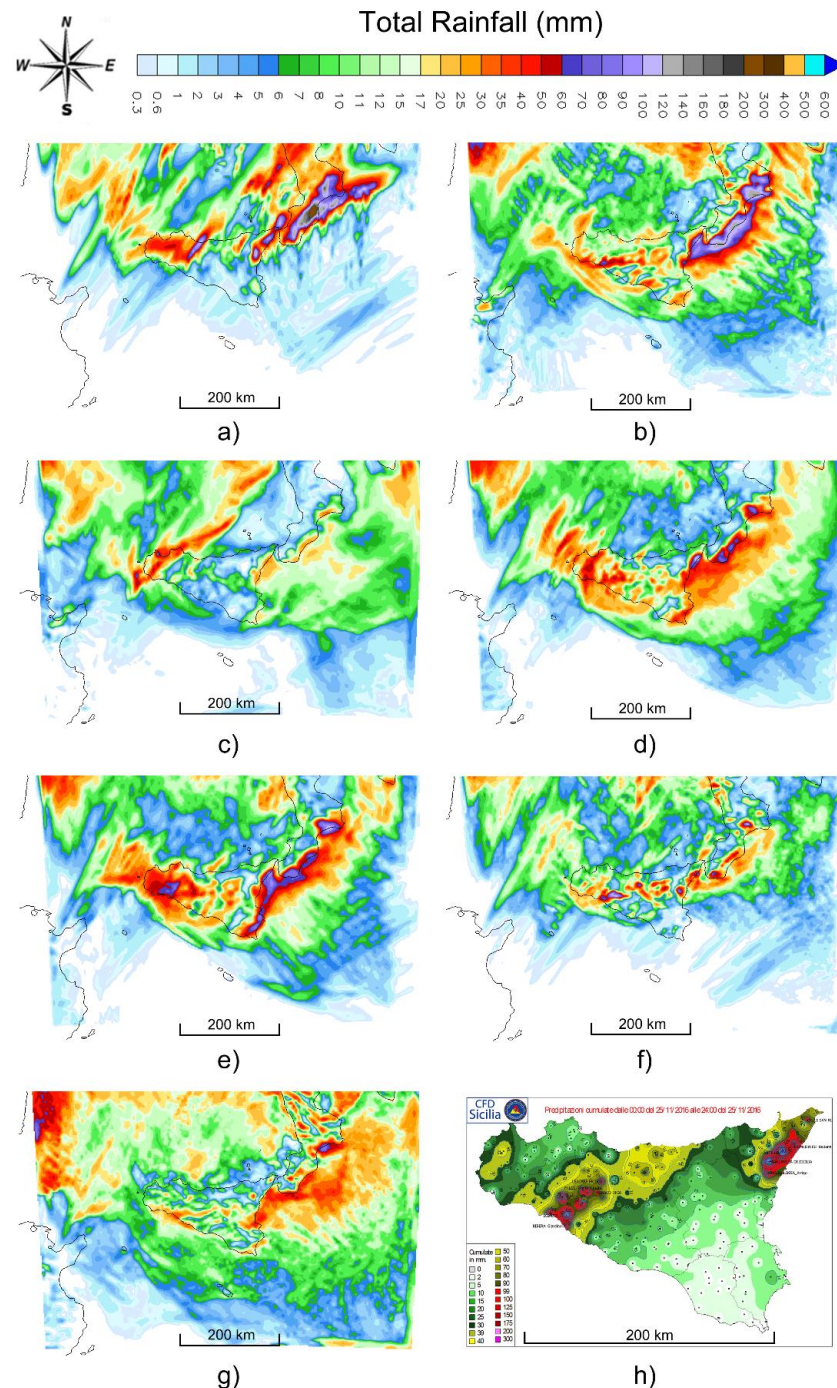


Figure 7. Total rainfall maps (accumulate + convective) obtained through the WRF model using different physical parametrizations of convective schemes and map of data observed by the DRPC weather stations network. (a) The CUO convective parameterization; (b) the CU1 convective parameterization; (c) the CU2 convective parameterization; (d) the CU3 convective parameterization; (e) the CU5 convective parameterization; (f) the CU6 convective parameterization; (g) the CU14 convective parameterization; (h) the map of a pluviometric data observation provided by the Regional Department of Civil Protection (DRPC) of Sicily.

However, visual analysis (called “Eyeball” verification) fails to show which physical parameterization of convective schemes provided the best performance. Furthermore, visual analysis is only a preliminary way to compare maps; it cannot be considered as a scientific approach for any comparison. Therefore, in order for us to evaluate which parameterization has provided the most reliable performance in predicting the spatial distribution of rain during the extreme event, the use of a statistical approach is fundamental. For this purpose, it is necessary to select a collection of weather stations in the area affected by the extreme event, as shown in Figure 8. The data of these stations are provided by the network of the Regional Department of Civil Protection (DRPC) of Sicily.

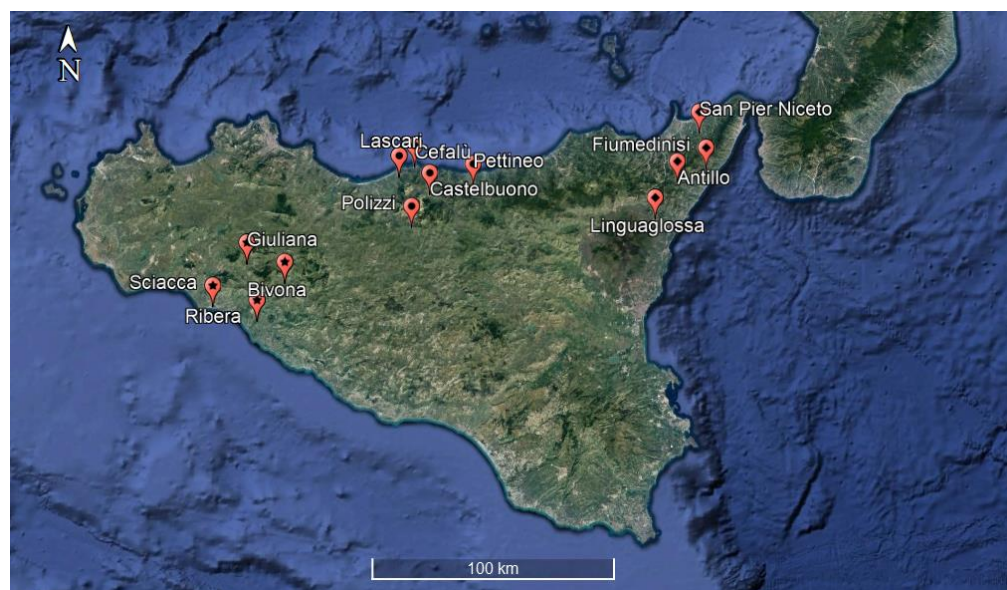


Figure 8. Map of weather stations used in this case study: 5 stations in the north of Sicily (Castelbuono, Lascari, Pettineo, Polizzi, and Cefalù), 4 in the northeast sector (Antillo, Fiumedinisi, Linguaglossa, and San Pier Niceto), and 4 in the southwest (Bivona, Giuliana, Ribera, and Sciacca).

To perform the analysis using the contingency table and calculate the indices reported in the next section, we needed to compare the data of the total rainfall observed (extrapolated from the DRPC-Sicily meteorological stations) with those predicted by the WRF model. Therefore, the extrapolation of the rainfall accumulations recorded by the 13 weather stations examined was carried out. The choice of weather stations was performed, accounting for the spatial localization of the extreme recorded meteorological event. The following stations were chosen as reference: five stations in the north of Sicily (Castelbuono, Lascari, Pettineo, Polizzi, and Cefalù), four in the northeast sector (Antillo, Fiumedinisi, Linguaglossa, and San Pier Niceto), and four in the southwest (Bivona, Giuliana, Ribera, and Sciacca). Subsequently, the rainfall data were extrapolated for each simulation in which the physical parametrizations of the convective phenomena were modified. The forecasted rainfall data and observed data by the 13 weather stations are shown in Tables 1–3.

The hour-by-hour time series of the pluviometric data forecast and observed for the weather stations of Bivona, Sciacca, Pettineo, and Fiumedinisi are shown as an example in the following graphs (Figure 9). The results show that the runs carried out with the WRF model underestimated the expected precipitation compared to that observed by the meteorological stations examined. This may have been due to the resolution of the model’s spatial grid; in fact, these meteorological events usually develop on smaller dimensions than the selected spatial grid. This could explain the underestimation of the total expected rainfall [20]. However, the spatial distribution and location of the meteorological event under consideration are well approximated by the simulations performed.

Table 1. The forecasted rainfall data and observed data provided by the 5 stations in the north of Sicily.

Stations in the North of Sicily	24 H Rain mm	24 H Rain mm CU0	24 H Rain mm CU1	24 H Rain mm CU2	24 H Rain mm CU3	24 H Rain mm CU5	24 H Rain mm CU6	24 H Rain mm CU14
Castelbuono	74.1	2.3	12.2	3	1.7	8.5	18.5	7.6
Lascari	53.6	15.7	14.5	3.6	11.1	12.6	7.5	5.3
Pettineo	46.2	10.5	17.9	2.5	3.7	2.8	8.8	7.2
Polizzi	89.4	8.2	7.5	1.1	7.1	7.3	8.2	0.8
Cefalù	34.1	8.1	19.1	3	23.6	25.7	16.3	6.2

Table 2. The forecasted rainfall data and observed data provided by the 5 stations in the northeast of Sicily.

Stations in the Northeast of Sicily	24 H Rain mm	24 H Rain mm CU0	24 H Rain mm CU1	24 H Rain mm CU2	24 H Rain mm CU3	24 H Rain mm CU5	24 H Rain mm CU6	24 H Rain mm CU14
Antillo	159.5	40.1	10.8	5.2	22.1	19.8	9.6	1.5
Fiumedinisi	153.8	71.3	26.5	10.8	40	15.3	18.1	2.1
Linguaglossa	92.1	50.1	1.4	0	2.1	0.5	0.4	1.2
San Pier Niceto	98.6	22	18.6	2.9	9.4	10.6	4.5	6.6

Table 3. The forecasted rainfall data and observed data provided by the 4 stations in the southwest of Sicily.

Stations in the Southwest of Sicily	24 H Rain mm	24 H Rain mm CU0	24 H Rain mm CU1	24 H Rain mm CU2	24 H Rain mm CU3	24 H Rain mm CU5	24 H Rain mm CU6	24 H Rain mm CU14
Bivona	64.3	29.1	52.5	6.6	53	39.3	102.6	53
Giuliana	163.2	33.3	39.0	9.8	41.3	29.3	53.6	53.6
Ribera	198.4	7.5	52.4	5	28.5	29.2	74.5	12.9
Sciacca	132.3	13.2	50.8	9.9	37.8	46.2	46.6	21

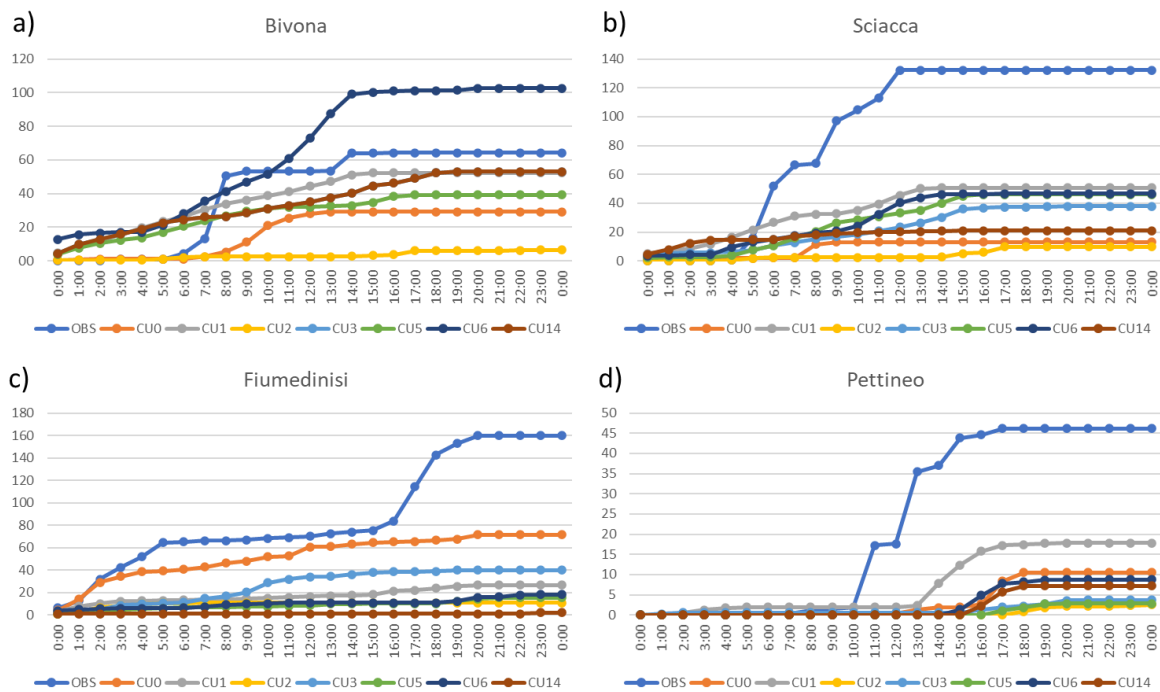


Figure 9. The hour-by-hour time series of the pluviometric data forecast and observed for the weather station. (a) The time series of the Bivona weather station; (b) the time series of the Sciacca weather station; (c) the time series of Fiumedinisi weather station; (d) the time series of the Pettineo weather station. In the graphs, the blue line represents the data observed by the weather station; the red line represents the simulation with the CU0 scheme; the green line represents the simulation with the CU1 scheme; the violet line represents the simulation with the CU2 scheme; the light blue line represents the simulation with the CU3 scheme; the orange line represents the simulation of the CU5 scheme; the dark blue line represents the simulation of the CU6 scheme; the burgundy line represents the simulation of the CU14 scheme.

4. Performance Testing of WRF Model Simulations

To establish which of the simulations provided the best performance, we needed to use statistical methods. The performance of a forecast model can be evaluated using one or more scalar verification indexes. A possible solution is provided by the dichotomic indexes, yes/no. To obtain them, we needed to place the data in a table of $I \times J$ elements, the so-called “contingency table”, which contains the absolute frequencies of all possible combinations of the observed and predicted data pairs. Considering the case $I = J = 2$, as shown in Figure 10, “a” indicates the number of cases in which the event was expected to occur and it is happening, “b” is the number of cases in which the event was expected to happen but it did not occur, “c” represents the number of cases in which the event occurred but was not expected, and finally “d” represents the number of cases in which the absence of the event was properly scheduled.

		Observed		
		yes	no	
Forecast	yes	a	b	a + b
	no	c	d	c + d
		a + c	b + d	N

Figure 10. Contingency table schedule. The term $a + b$ represents the forecasted meteorological events by the model. The term $c + d$ represents the not forecasted meteorological events by the model. The term $a + c$ represents the observed rainy weather events. The term $a + d$ represents the non-observed rainy weather events.

Dividing by $N = a + b + c + d$, we obtained the combined distribution of prediction relative frequencies and the observed data; a perfect forecast has non-zero values only for the elements on the diagonal of the table.

From the contingency table, we were able to define the categorical indexes used to quantify the yield of the simulations performed with this model, in particular:

- Accuracy (Hit rate): defined as the ratio between the number of cases in which the event was correctly predicted and the total number of cases considered (n). The value 0 indicates a bad forecast, the value 1 indicates a perfect forecast.
- Threat score (TS): an alternative to the hit rate, useful when the event considered has a substantially lower occurrence frequency than non-occurrence. If the threat score assumes the value 0, the forecast will be bad; otherwise, if it assumes the value 1, the forecast will be perfect.
- Bias: represents the ratio between the predicted and observed data average.
 $B = 1 \rightarrow$ the event was predicted the same number of times that it was observed.
 $B > 1 \rightarrow$ over forecasting, the model predicts events with greater frequency than reality.
 $B < 1 \rightarrow$ under forecasting, the model predicts events with a lower frequency than reality.
- False alarms ratio (FAR): illustrates that the model has made a forecast of rainfall for the valid period but it did not occur during the valid period. It is especially useful to verify the prediction ability of extreme events. If it assumes the value 0, the forecast will be perfect; if it assumes value 1, there will be the prediction of events that will not happen.
- Equitable threat score (ETS): based on TS; by definition ranging from $-1/3$ to 1 (perfect prediction).
- Hanssen–Kuipers discriminant: given by the ratio between the events correctly predicted and those actually occurred less the probability of having a false alarm. By definition ranging from -1 to 1 (perfect prediction).
- Probability of detection (POD): sensitive to hits, but ignores false alarms. Very sensitive to the climatological frequency of the event. Good for rare events. Should be used

in conjunction with the FAR. Its range is between 0 and 1; if it assumes the value 1, the forecast will be perfect.

Table 4 and Figure 11 show the numerical values obtained from the statistical analysis carried out to evaluate which simulation provided the best performance in locating the meteorological event under consideration. It should be noted that the contingency table shows the frequency of “yes” and “no” forecasts and occurrences. No comparison or evaluation is made on the expected and observed quantities of pluviometric data.

Table 4. Numeric values of indexes were calculated for each simulation performed by modifying the physical parameterization of the convective processes of the WRF model. For the analysis, all the selected meteorological stations and the respective points of the WRF model were taken into consideration. The ideal values are: accuracy (hit rate) = 1; threat score (TS) = 1; bias = 1; equitable threat score (ETS) = 1; probability of detection (POD) = 1; false alarms ratio (FAR) = 0.

	CU0	CU1	CU2	CU3	CU5	CU6	CU14
Accuracy	0.68	0.53	0.45	0.54	0.53	0.51	0.52
TS	0.49	0.43	0.12	0.38	0.35	0.30	0.26
Bias	0.95	1.47	0.49	1.13	1.07	0.91	0.73
ETS	0.22	0.04	-0.06	0.05	0.03	0.01	0.01
POD	0.64	0.74	0.16	0.58	0.54	0.44	0.36
FAR	0.33	0.50	0.67	0.48	0.50	0.51	0.51

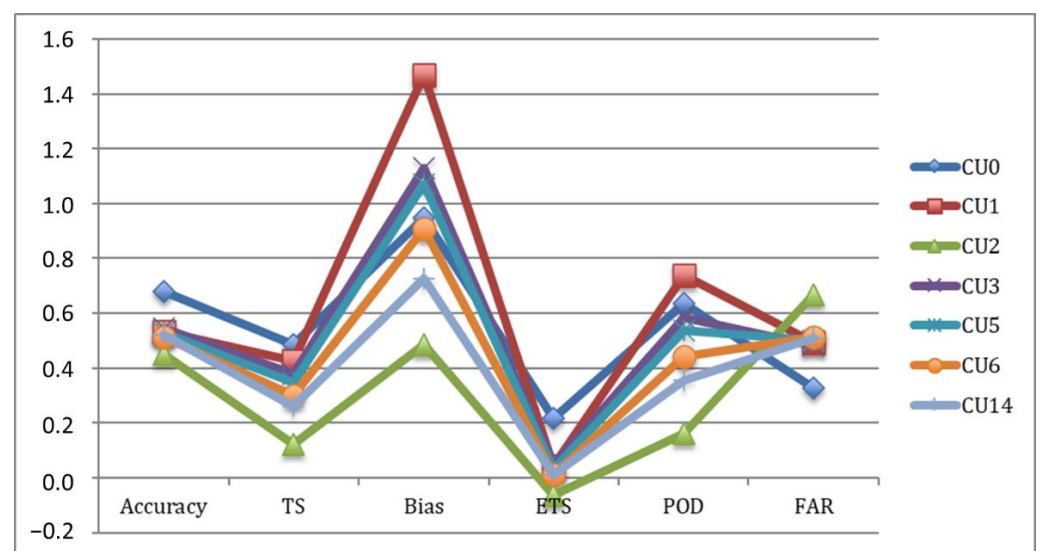


Figure 11. Graphic of indexes calculated for each simulation performed by modifying the physical parameterization of the convective processes of the WRF model. It shows that the CU0 (blue line) was the most reliable and accurate solution. The CU2 (green line) was the worst. CU1 (red line), CU3 (violet line), and CU5 (light blue line) were the only schemes that tended to overestimate the rain. The CU14 and the CU6 (orange line) schemes were only slightly better than the CU2. The CU14 and the CU6 (orange line) schemes were only slightly better than the CU2.

The analysis shows that the explicit resolution of convective processes (CU0) was the most reliable and accurate solution with the highest accuracy in terms of threat score and equitable threat score.

The Betts–Miller–Janic scheme (CU2) was the worst and was the one that also generated the highest number of false alarms (FARs). The new simplified Arakawa–Schubert (CU14) and Tiedtke (CU 6) schemes were only slightly better than the BMJ (CU2). The new Kain–Fritsch (CU1), the Grell–Devenyi (CU3), and the Grell 3D (CU 5) schemes were the only schemes that tended to overestimate the rain. The new Kain–Fritsch scheme (CU1),

except for an excessive BIAS overlapping, was found to have good overall behavior and was the one that showed the maximum POD (probability of detection).

5. Conclusions

The physical parameterization of the convective schemes plays a fundamental role in optimizing the performance of limited area meteorological models, especially in cases of extreme meteorological events. In the case study investigated, the goal was to evaluate which simulation provided the best performance in spatially locating an extreme event as a function of the physical parameterization of the convective patterns. For this purpose, we considered the extreme event recorded in Sicily on 25 November 2016 as a case study.

It was shown that the only evaluation by visual analysis (called “Eyeball” verification) was not sufficient to establish which simulation was the best performing. Therefore, a statistical study through the use of the contingency table was found to be fundamental. The study highlighted that the explicit resolution of the convective schemes (CU0) provided the best simulation for the spatial forecast of the extreme meteorological event. This result was expected from the literature, because most convective clouds have horizontal dimensions ranging from 0.1 to 10 km, generally smaller than those of the spatial grid of the limited area model (5 km) used in this case study (typical sub-grid phenomenon).

Author Contributions: All authors contributed to conceptualization, methodology, investigation, writing, reviewing, and editing of the present work. Writing—review & editing, G.C., M.T.C., F.C. and S.M. All authors have read and agreed to the published version of the manuscript.

Funding: This work is to be framed within the Progetto di Ricerca e Sviluppo “Impiego di tecnologie, materiali e modelli innovativi in ambito aeronautico (AEROMAT)”, Asse II “Sostegno all’innovazione”, Area di Specializzazione “Aerospazio” Avviso n. 1735/Ric del 13 luglio 2017—Codice CUP J66C18000490005, codice identificativo Progetto ARS01_01147 nell’ambito del Programma Operativo Nazionale “Ricerca e Innovazione” 2014–2020 (PON R&I 2014–2020).

Institutional Review Board Statement: Not applicable.

Informed Consent Statement: Not applicable.

Data Availability Statement: Not applicable.

Acknowledgments: The authors wish to acknowledge the Regional Department of Civil Protection (DRPC) of Sicily and the Italian Air Force Meteorological Service for the observed rainfall data and maps provided.

Conflicts of Interest: The authors declare no conflict of interest.

References

1. Cassola, F.; Ferrari, F.; Mazzino, A. Numerical simulations of Mediterranean heavy precipitation events with the WRF model: A verification exercise using different approaches. *Atmos. Res.* **2015**, *164–165*, 210–225. [CrossRef]
2. Caccamo, M.T.; Castorina, G.; Catalano, F.; Magazù, S. Ruchardt’s experiment treated by Fourier Transform. *Eur. J. Phys.* **2019**, *40*, 025703. [CrossRef]
3. Castorina, G.; Caccamo, M.T.; Magazù, S. A new approach to the adiabatic piston problem through the arduino board and innovative frequency analysis procedures. In *New Trends in Physics Education Research*; Nova Science Publishers, Inc.: Hauppauge, NY, USA, 2018; pp. 133–156.
4. Anthes, R.A. Regional Models of the atmosphere in the middle latitudes. *Mon. Weather Rev.* **1983**, *111*, 1306–1335. [CrossRef]
5. Lackman, G. *Mid-Latitude Synoptic Meteorology*; American Meteorological Society: Boston, MA, USA, 2011.
6. Markowski, P.; Richardson, Y. *Mesoscale Meteorology in Mid-latitudes*; Wiley: Hoboken, NJ, USA, 2010.
7. Altinbilek, D.; Barret, E.C.; Oweis, T.; Salameh, E.; Siccardi, F. Rainfall Climatology on the Mediterranean in EU-AVI 080 Project across—Analyzed Climatology Rainfall Obtained from Satellite and Surface Data in the Mediterranean Basin. 1997. Available online: <http://www.diam.unige.it/idromet/avi080/altinb.html> (accessed on 15 February 2021).
8. Martin, J.E. *Mid-Latitude Atmospheric Dynamics. A First Course*; Wiley: Hoboken, NJ, USA, 2006.
9. Miglietta, M.M.; Buzzi, A. A numerical study of moist stratified flows over isolated topography. *Tellus A* **2001**, *53*, 481–499. [CrossRef]
10. Davolio, S.; Buzzi, A.; Malguzzi, P. Orographic influence on deep convection: Case study and sensitivity experiments. *Meteorol. Z.* **2006**, *15*, 215–223. [CrossRef]

11. Chu, C.; Lin, Y. Effects of orography on the generation and propagation of mesoscale convective systems in a two-dimensional unstable flow. *J. Atmos. Sci.* **2000**, *57*, 3817–3837. [[CrossRef](#)]
12. Anthes, R.A.; Kuo, Y.-H.; Hisie, E.-Y.; Low-Nam, S.; Bettge, T.W. Estimation of skill and uncertainty in regional numerical models. *Q. J. R. Meteorol. Soc.* **1989**, *115*, 763–806. [[CrossRef](#)]
13. Castorina, G.; Caccamo, M.T.; Magazù, S. Study of convective motions and analysis of the impact of physical parametrization on the wrf-arw forecast model. *Atti Accad. Peloritana Pericolanti Cl. Sci. Fis. Mat. Nat.* **2019**, *97*, A19. [[CrossRef](#)]
14. Randall, D. *An Introduction to Atmospheric Modelling*; Department of Atmospheric Science, Colorado State University: Boulder, CO, USA, 2001.
15. Kalnay, L. *Atmospheric Modeling, Data Assimilation and Predictability*; Cambridge University Press: Cambridge, UK, 2002.
16. Rizza, U.; Miglietta, M.M.; Mangia, C.; Ielpo, P.; Morichetti, M.; Iachini, C.; Virgili, S.; Passerini, G. Sensitivity of WRF-Chem model to land surface schemes: Assessment in a severe dust outbreak episode in the Central Mediterranean (Apulia Region). *Atmos. Res.* **2018**, *201*, 168–180. [[CrossRef](#)]
17. Rizza, U.; Brega, E.; Caccamo, M.T.; Castorina, G.; Morichetti, M.; Munaò, G.; Passerini, G.; Magazù, S. Analysis of the ETNA 2015 Eruption Using WRF–Chem Model and Satellite Observations. *Atmosphere* **2020**, *11*, 1168. [[CrossRef](#)]
18. Castorina, G.; Caccamo, M.T.; Magazù, S.; Restuccia, L. Multiscale mathematical and physical model for the study of nucleation processes in meteorology. *Atti Accad. Peloritana Pericolanti Cl. Sci. Fis. Mat. Nat.* **2018**, *96*. [[CrossRef](#)]
19. Skamarock, W.C. *A Description of the Advanced Research WRF Version 3* NCAR; Technical Note; University Corporation for Atmospheric Research: Boulder, CO, USA, 2008.
20. Caccamo, M.T.; Castorina, G.; Colombo, F.; Insinga, V.; Maiorana, E.; Magazù, S. Weather forecast performances for complex orographic areas: Impact of different grid resolutions and of geographic data on heavy rainfall event simulations in Sicily. *Atmos. Res.* **2017**, *198*, 22–33. [[CrossRef](#)]
21. Castorina, G.; Colombo, F.; Caccamo, M.T.; Cannuli, A.; Insinga, V.; Maiorana, E.; Magazù, S. Cultural Heritage and Natural Hazard: How WRF Model Can Help to Protect and Safe Archaeological Sites. *Int. J. Res. Environ. Sci.* **2017**, *3*, 37–42. [[CrossRef](#)]
22. Colombo, F.; Castorina, G.; Caccamo, M.T.; Insinga, V.; Maiorana, E.; Magazù, S. IT Technologies for Science Application: Using meteorological Local Area Model to Contrast the Hydrogeological Risks. *Hydrol. Curr.* **2017**, *8*, 1000284.
23. Smith, R. The influence of mountains on the atmosphere. *Adv. Geophys.* **1979**, *21*, 87–230.
24. Wallace, J.M.; Hobbs, P.V. *Atmospheric Science: An Introductory Survey*; Academic Press: Cambridge, MA, USA, 2006.
25. Kuo, H.L. Further studies of the parameterization of the effect of cumulus convection on large scale flow. *J. Atmos. Sci.* **1974**, *31*, 1232–1240. [[CrossRef](#)]
26. Emanuel, K.A.; Raymond, D.J. *The Representation of Cumulus Convection in Numerical Models*; Springer: Berlin/Heidelberg, Germany, 1993.
27. Haltiner, G.; Williams, H. *Numerical Prediction and Dynamic Meteorology*; Wiley Sons Ltd.: Hoboken, NJ, USA, 1983.
28. Stensrud, D.J. *Parametrization Scheme*; Cambridge University Press: Cambridge, UK, 2007.
29. Reeves, H.D.; Rotunno, R. Orographic flow response to variations in upstream humidity. *J. Atmos. Sci.* **2008**, *66*, 3557–3570. [[CrossRef](#)]
30. Salby, M.L. *Fundamentals of Atmospheric Physics*; Academic Press: Cambridge, MA, USA, 1996.
31. Pielke, R.A.; Pearce, R.P. *Mesoscale Modeling of the Atmosphere*; American Meteorological Society: Boston, MA, USA, 1994.
32. Ray, P. *Mesoscale Meteorology and Forecasting*; American Meteorological Society: Boston, MA, USA, 1986.
33. Anthes, R.A. A cumulus parameterization scheme utilizing a one dimensional cloud model. *Mon. Weater. Rev.* **1977**, *105*, 270–286. [[CrossRef](#)]
34. Kain, J.S.; Fritsch, J.M. The role of trigger function in numerical forecasts of mesoscale convective system. *Meteorol. Atmos. Phys.* **1992**, *49*, 93–106. [[CrossRef](#)]
35. Kain, J.S. The Kain–Fritsch convective parameterization: An update. *J. Appl. Meteorol.* **2004**, *43*, 170–181. [[CrossRef](#)]
36. Betts, A.K. A new convective adjustment scheme. Part I. Observational and theoretical basis. *Q. J. R. Meteorol. Soc.* **1986**, *112*, 677–691.
37. Betts, A.K.; Miller, M.J. A new convective adjustment scheme. Part II. Single column tests using GATE wave, BOMEX, ATEX and arctic air-mass data sets. *Q. J. R. Meteorol. Soc.* **1986**, *112*, 693–709.
38. Fritsch, J.M.; Chappel, C.F. Numerical prediction of convectively driven mesoscale pressure system. Part I: Convective parameterization. *J. Atmos. Sci.* **1890**, *37*, 1722–1733. [[CrossRef](#)]
39. Arakawa, A.; Schubert, W.H. Interaction of a cumulus cloud ensemble with the large scale environment. *Part I*. *J. Atmos. Sci.* **1974**, *31*, 674–701. [[CrossRef](#)]